Direct Measurement of the Nickel Spectrum in Cosmic Rays in the Energy Range from 8.8 GeV/n to 240 GeV/n with CALET on the International Space Station

SUPPLEMENTAL MATERIAL

(CALET collaboration)

Supplemental material relative to "Direct Measurement of the Nickel Spectrum in Cosmic Rays in the Energy Range from 8.8 GeV/n to 240 GeV/n with CALET on the International Space Station with the Calorimetric Electron Telescope".

ADDITIONAL INFORMATION ON THE ANALYSIS

Charge measurement. The particle's charge Z is reconstructed from the ionization deposits in the CHD paddles traversed by the incident particle. Either CHD layer provides an independent dE/dx measurement which is corrected for the track path length and for the quenching effect in the scintillator's light yield as a function of Z^2 (Refs. [S1, S2]). In Fig. S1 inclusive distributions of measured charges from flight data (FD) are compared, in two different energy bins, with Monte Carlo (MC) simulations from EPICS.
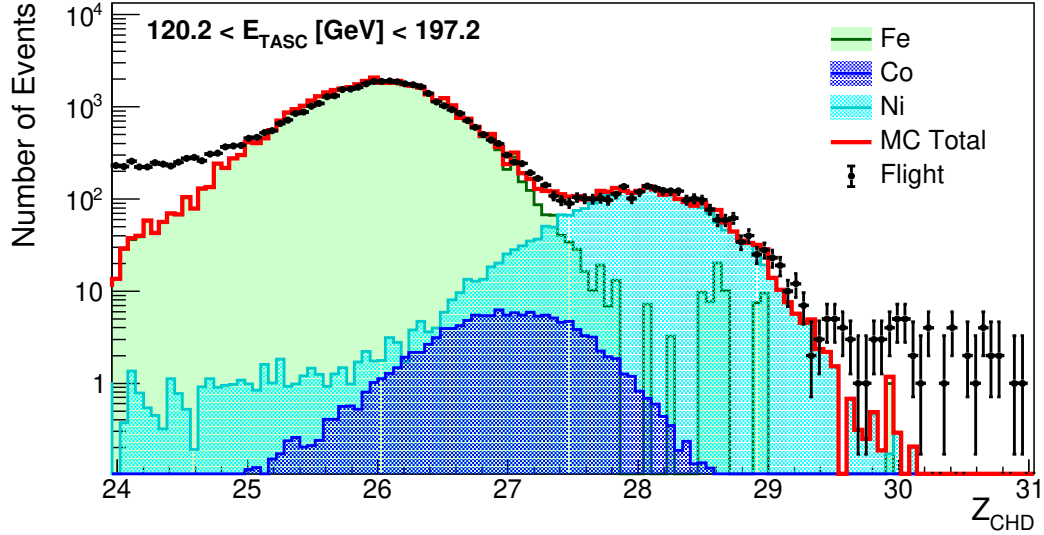
(a)
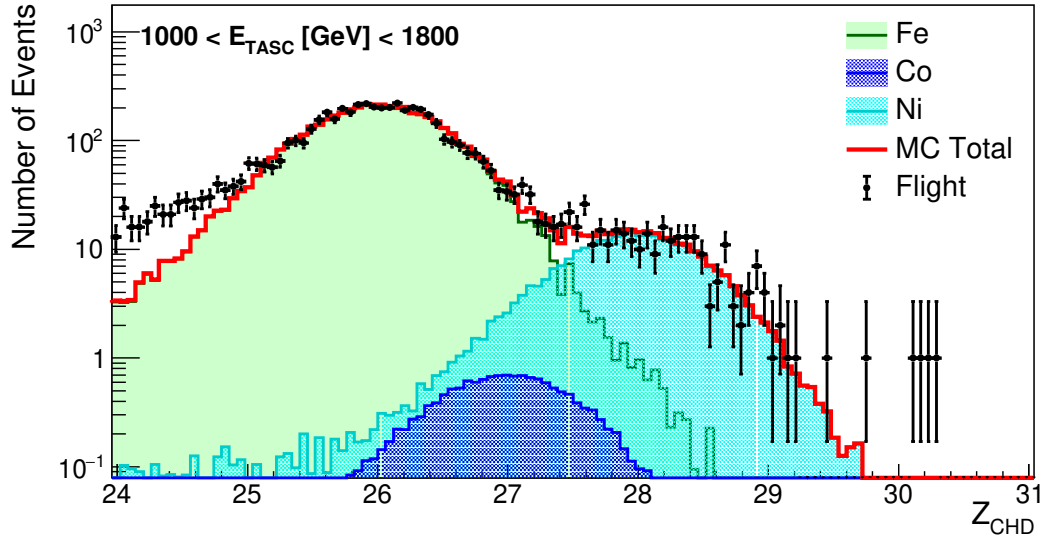
(b)

FIG. S1. Charge distributions from the combined charge measurement of the two CHD layers in the elemental region between Cr and Ga. Events are selected with $120.2 < E_{TASC} < 197.2$ GeV in (a) and $1000 < E_{TASC} < 1800$ GeV in (b). Flight data, represented by black dots, are compared with Monte Carlo samples including iron, cobalt and nickel. Chromium, manganese and nuclei with $Z \geq 29$ are not included in MC because their contamination to nickel data is negligible.

Background contamination. Background contamination of nickel from neighbor elements is relatively small between 100 GeV and 1 TeV mainly due to iron and secondly to cobalt. Above 1 TeV the iron contribution becomes important and exceeds 10% above 10 TeV. The distribution of nickel candidates and its contaminants is shown in Fig. S2 as a function of the TASC energy. The total contamination (estimated by fitting a constant up to 1.7 TeV and a first order logarithmic polynomial up to 20 TeV) was subtracted from the flux as explained in the main body of the paper.

To evaluate the systematic error related to the background, the constant parameter of the fit was varied by as much as twice its error. This resulted into a $\pm 50\%$ variation of the contamination with a negligible change of the flux (see main body).
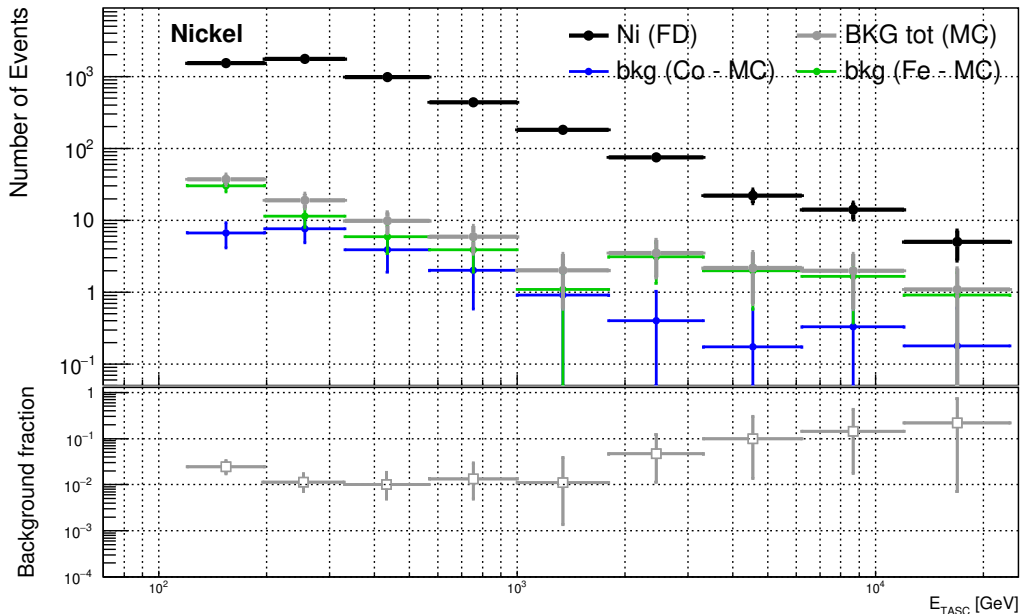

FIG. S2. Top panel: Differential distributions of the number of events in a given bin of calorimetric energy (E_{TASC} in GeV) for selected nickel events in flight data (black dots) before the unfolding procedure and with background events from iron and cobalt nuclei. Bottom panel: Contamination from Fe and Co obtained with the MC. The Monte Carlo events are weighted with a factor to reproduce a single power law spectrum with spectral index -2.6, and event selection is the same as for flight data. The resulting elemental charge distribution in each observed energy bin has been normalized to match the CHD charge distribution of flight data. The number of contaminant events is calculated by integration of all the MC events retained by the nickel charge selection.

Efficiencies. The total efficiency and relative efficiencies (i.e., the efficiency of a given cut normalized to the previous cut) were studied extensively over the whole energy range covered by the nickel flux measurement. The total selection efficiency from EPICS (red filled circles) and GEANT4 (blue filled circles) are shown in Fig. S3 as a function of total particle kinetic energy per nucleon. The above efficiencies were validated by comparing distributions relevant to the selection of events, and obtained from flight data, with the same distributions generated by EPICS or GEANT4.

TASC energy deposits. An example is given in Fig. S4 where the total energy observed in each layer of the TASC (black points) was plotted using the final sample of nickel candidates, marginally contaminated by a residual background due to elements with atomic number close to nickel. Compared with pure nickel samples simulated by EPICS (red) or GEANT4 (blue), the distributions from the two MC were found to be consistent with each other and in fair agreement with flight data.

Interactions in the instrument. The amount of instrument material above the CHD is very small and well known. The largest significant contribution is limited to a 2 mm thick Al cover placed on top of the CHD. This amounts to $\sim 2.2\%$ radiation length and 5×10^{-3} proton interaction lengths (λ_I). The material description in the MC is very accurate and derived directly from the CAD model. As CALET is sitting on the JEM external platform of the ISS, no extra material external to CALET is normally present within the acceptance for the flux measurement. However, occasional obstructions caused by the ISS robotic arm operations may temporarily affect the field of view (FOV). It was checked that removing those rare periods from the flux results in a negligible difference in shape and normalization (<1%).

MC simulations were used to evaluate the nickel survival probability after traversing both layers of the CHD and the material above. In order to check its consistency with flight data, the ratio R = (CHDX & CHDY) / CHDX (i.e.
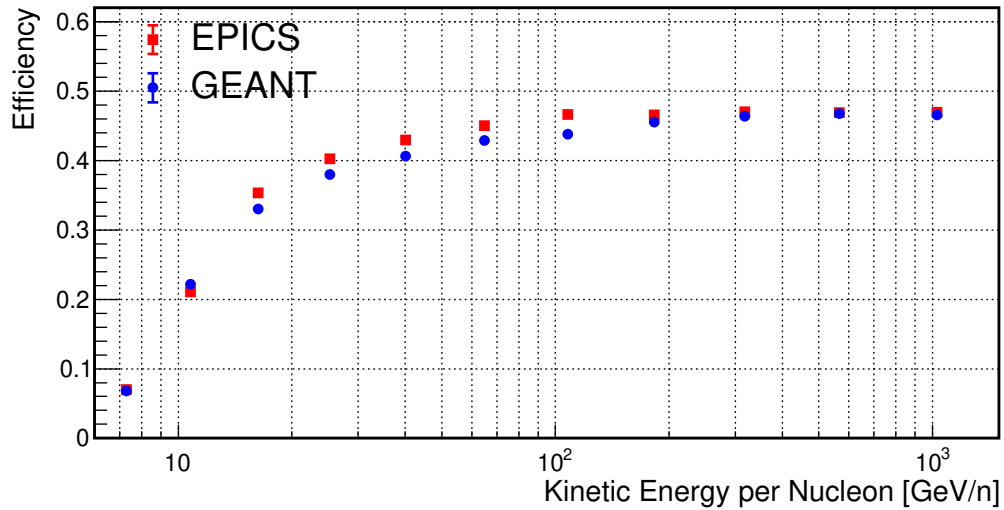
FIG. S3. Total selection efficiency for nickel events as estimated with EPICS (red filled circles) and GEANT4 (blue filled circles) simulations.
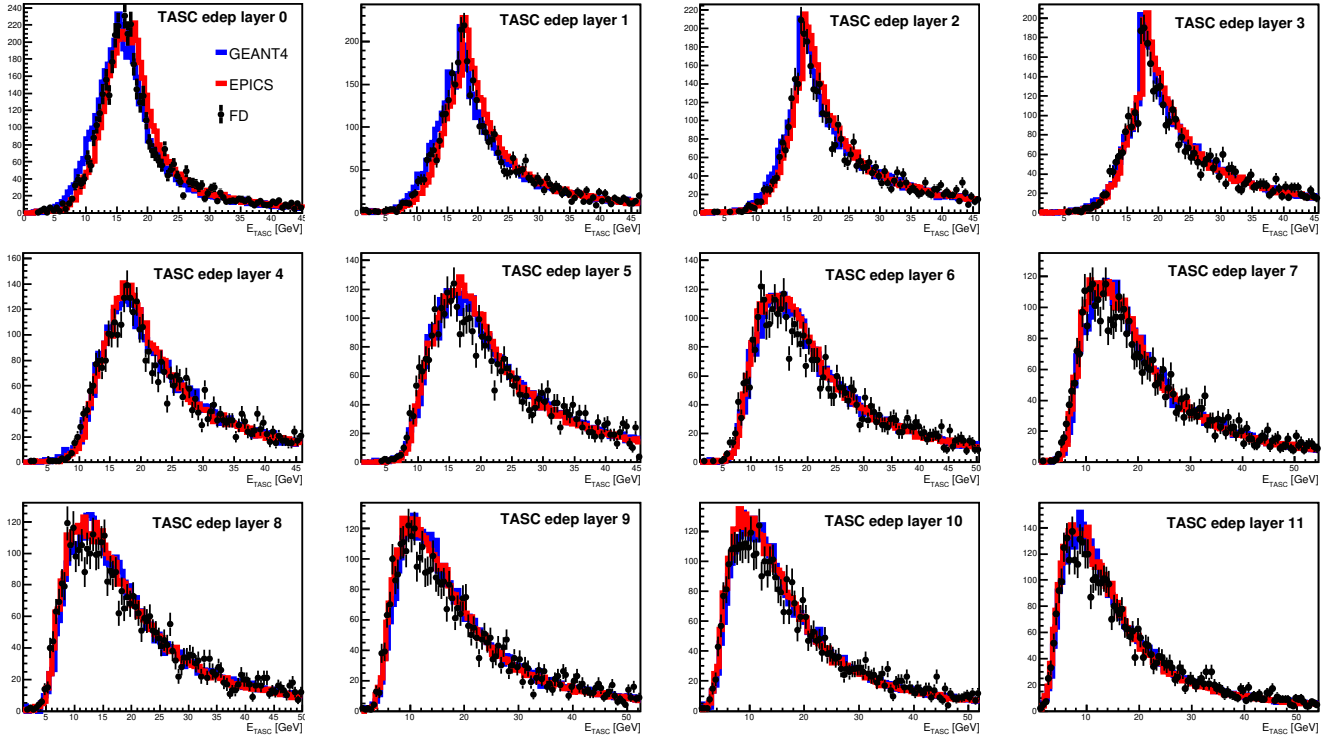

FIG. S4. Energy observed in each of the 12 layers of the TASC (black points) for the final sample of nickel candidates from flight data. It is compared with pure samples of nickel simulated by EPICS (red) or GEANT4 (blue).

the fraction of nickel candidates tagged by both CHD layers among those detected by the top charge detector alone) was plotted, as a function of the TASC energy, for selected nickel candidates with measured charge in the range 27.7 - 28.3 charge units. In the upper panel of Fig. S5, R is shown in 8 bins of the TASC energy for both MC (R_{MC}) and FD (R_{FD}) with an average value around 90% and a flat energy dependence. The R_{MC}/R_{FD} *double ratio* (lower plot) shows a good level of consistency between the MC and flight data, within the errors. The total loss ($\sim 10\%$) of nickel events interacting in the upper part of the instrument was taken into account in the total efficiency and its uncertainty included in the systematic error.
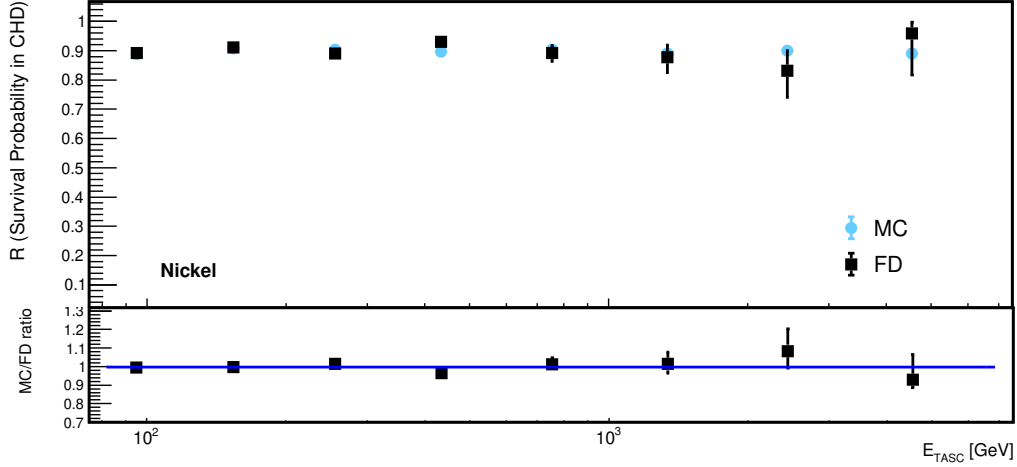
FIG. S5. Top panel: nickel survival probability R as a function of energy for events crossing both layers of the CHD with flight data (black filled squares) and EPICS (blue filled circles); Bottom panel: ratio of R_{MC}/R_{FD} with the MC and flight data, respectively, fitted with a constant and consistent with unity within the error.

Calorimetric energy, **bin size**, **and unfolding**. The energy response of the TASC was studied with MC simulations and compared with the results of measurements of the total particle energy vs beam momentum carried out at CERN. During one of the beam test campaigns of CALET at the SPS with an extracted primary beam of ^{40}Ar (150 GeV/c/n), beam fragments were generated from an internal target and guided toward the instrument along a magnetic beam spectrometer that provided an accurate selection of their rigidity and A/Z ratio. The relation between the observed TASC energy and the primary energy was measured for several nuclei up to the highest available energy (6 TeV total particle energy in the case of ^{40}Ar). After an offline rejection of a very small amount of beam contaminants from the data, the shape of the TASC total energy was found to be consistent with a Gaussian distribution (Ref. [S3]).

The correlation matrix used for the unfolding was derived from the simulations, using two different MC codes EPICS and GEANT4, and applying the same selection cuts as in the FD analysis. The normalized unfolding matrices obtained from EPICS and GEANT4 are shown in Fig. S6 where the color scale indicates the probability for a nickel candidate, with a given primary energy, of depositing energy in different intervals of E_{TASC}.
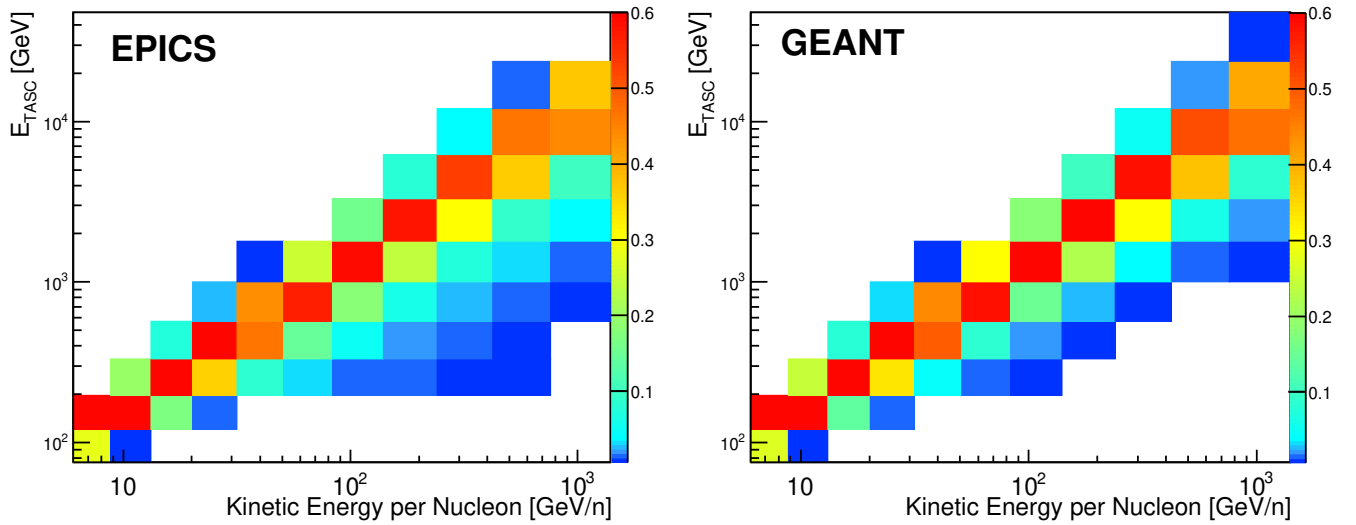

FIG. S6. Response matrix for nickel derived from the MC simulations of the CALET flight model by applying the same selection as for flight data. The array is normalized so that the color scale is associated with the probability that nickel candidates, in a given bin of particle kinetic energy, migrate to different intervals of E_{TASC}. Left: EPICS; Right: GEANT4.

A standard binning scheme, consisting of smoothly enlarged bins, was chosen in order to balance the statistical population at high energy without using too large consecutive bins. In order to investigate the effect of the binning choice, different binning configurations (3 bins per decade, 4 bins per decade and 5 bins per decade) were tested, obtaining similar smearing matrices and almost identical behavior in the final flux. As an example, the difference between the flux with the standard binning and with 4 bins per decade is shown in Fig. S7.
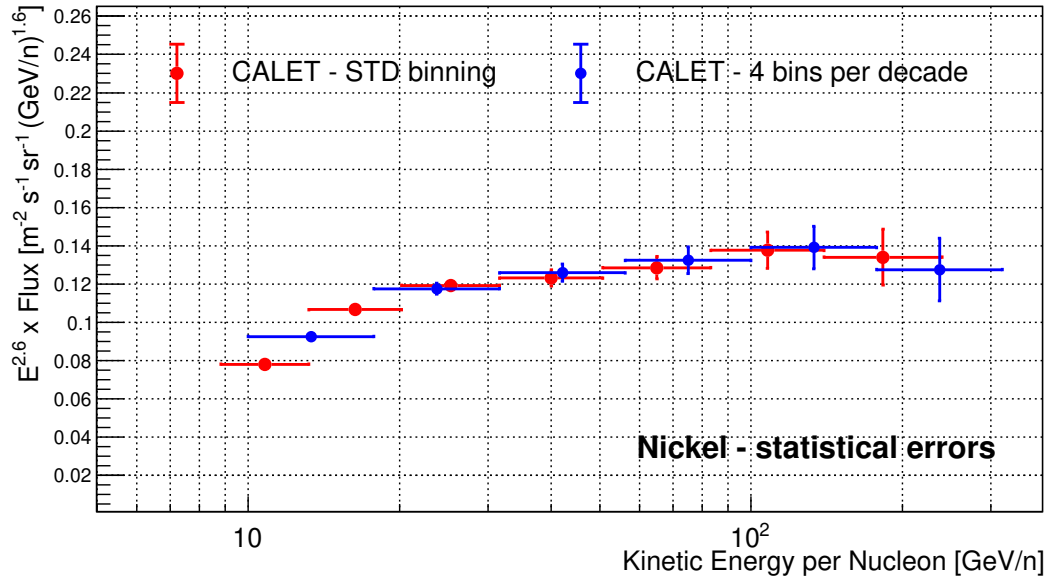

FIG. S7. CALET nickel flux with standard binning (red circles) and 4 bins/decade (blue circles). The vertical error bars are representative of purely statistical errors whereas the horizontal ones indicate the bin width.

Energy dependent systematic errors. A breakdown of energy dependent systematic errors stemming from several sources (as explained in the main body of the paper) and including selection cuts, charge identification, MC model, energy scale correction, energy unfolding, beam test configuration and shower event shape is shown in Fig. S8 as a function of kinetic energy per nucleon.

Nickel flux normalization and spectral shape. The CALET nickel flux and a compilation of available data are shown in Fig. S9, as an enlarged version of Fig. 2 in the main body of the paper.
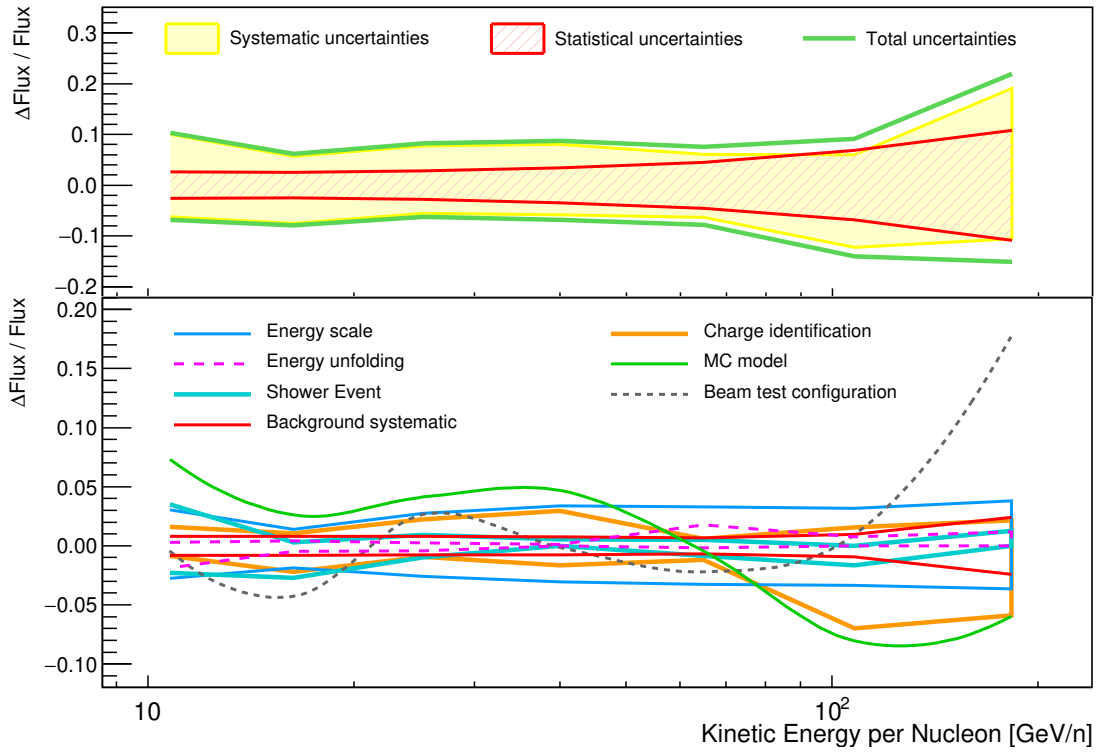
FIG. S8. Energy dependence (in GeV/nucleon) of systematic uncertainties (relative errors) for nickel. In the upper panel, the band bounded by the red lines represents the statistical error. The yellow band shows the sum in quadrature of all the sources of systematics including energy independent ones. The green lines represent the sum in quadrature of statistical and total systematic uncertainties. In the bottom panel, a detailed breakdown of systematic energy dependent errors, stemming from charge identification, MC model, energy scale correction, energy unfolding, beam test configuration and shower event shape is shown.
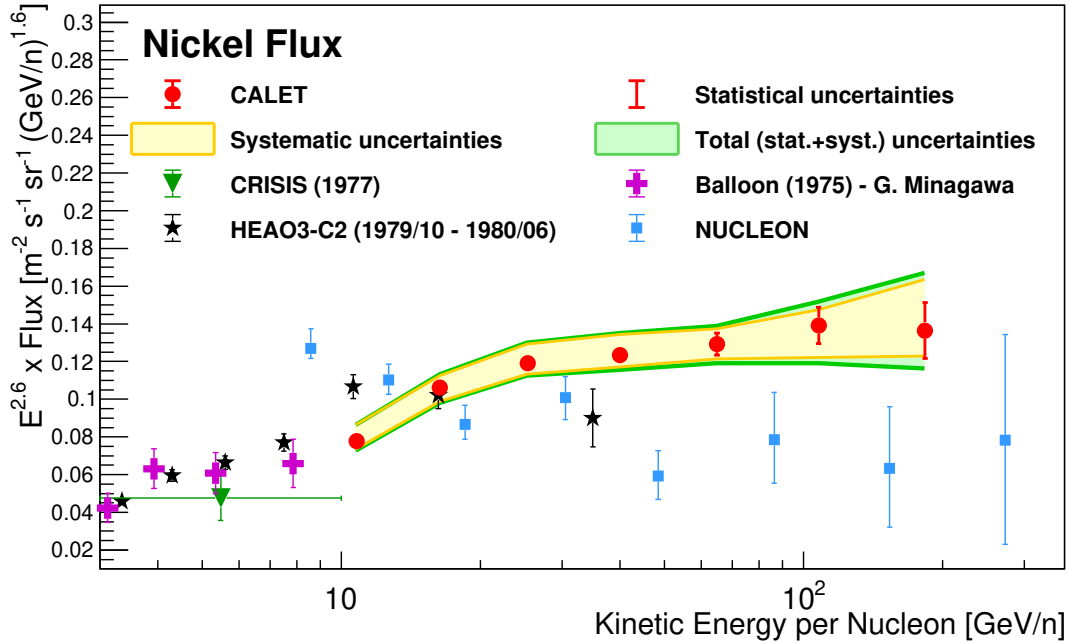

FIG. S9. CALET nickel flux as a function of kinetic energy per nucleon in GeV (with multiplicative factor $E^{2.6}$). The error bars of the CALET data (red filled circles) represent the statistical uncertainty only. The yellow band indicates the quadrature sum of systematic errors, while the green band indicates the quadrature sum of statistical and systematic errors. Also plotted are the data points from Balloon 1975 [S4], CRISIS [S5], HEAO3-C2 [S6] and NUCLEON [S7].

TABLE I. Table of the CALET differential spectrum in kinetic energy per nucleon of cosmic-ray nickel. The first, second, and third error in the flux are representative of the statistical uncertainties, systematic uncertainties in normalization, and energy dependent systematic uncertainties, respectively.

Energy Bin [GeV/n]	Flux [m^{-2}sr^{-1}s^{-1}(GeV/n)$^{-1}$]
$8.8 - 13.2$	$(1.61 \pm 0.04 \, ^{+0.07}_{-0.08} \, ^{+0.14}_{-0.07}) \times 10^{-4}$
$13.2 - 20.2$	$(7.48 \pm 0.19 \, ^{+0.35}_{-0.38} \, ^{+0.24}_{-0.45}) \times 10^{-5}$
$20.2 - 31.6$	$(2.69 \pm 0.08 \, ^{+0.12}_{-0.14} \, ^{+0.19}_{-0.06}) \times 10^{-5}$
$31.6 - 50.7$	$(8.41 \pm 0.29 \, ^{+0.39}_{-0.43} \, ^{+0.59}_{-0.25}) \times 10^{-6}$
$50.7 - 83.2$	$(2.51 \pm 0.11 \, ^{+0.12}_{-0.13} \, ^{+0.09}_{-0.12}) \times 10^{-6}$
$83.2 - 139,6$	$(7.23 \pm 0.50 \, ^{+0.33}_{-0.37} \, ^{+0.20}_{-0.85}) \times 10^{-7}$
$139.6 - 239.9$	$(1.79 \pm 0.19 \, ^{+0.08}_{-0.09} \, ^{+0.33}_{-0.16}) \times 10^{-7}$

[S1] P. S. Marrocchesi *et al.*, Nucl. Instr. and Meth. A **659**, 477 (2011).
[S2] O. Adriani (CALET), Phys. Rev. Lett. **125**, 251102 (2020).
[S3] Y. Akaike (CALET), in *Proceedings of Science (ICRC2015) 613* (2015).
[S4] G. Minagawa, Astrophys. J. **248**, 847 (1981).
[S5] J. S. Young *et al.*, Astrophys. J. **246**, 1014 (1981).
[S6] J. J. Engelmann *et al.* (HEAO3-C2), Astron. Astrophys. **233**, 96 (1990).
[S7] V. Grebenyuk *et al.* (NUCLEON), (2018), arXiv:1809.07285 [astro-ph.HE].